Faraday Discussions

The interplay between snow and polluted air masses in cold urban environments

Journal:	*Faraday Discussions*
Manuscript ID	FD-ART-11-2024-000176.R1
Article Type:	Paper
Date Submitted by the Author:	07-Dec-2024

Complete List of Authors:	Kuhn, Jonas; University of California Los Angeles, Department of Atmospheric and Oceanic Sciences Stutz, Jochen; University of California Los Angeles, Department of Atmospheric and Oceanic Sciences Bartels-Rausch, Thorsten; Paul Scherrer Institut PSI, Laboratory of Atmospheric Chemistry Thomas, Jennie; University Grenoble Alpes Cesler-Maloney, Meeta; University of Alaska Fairbanks, Chemistry & Biochemistry Simpson, William; University of Alaska Fairbanks, Chemistry & Biochemistry Dibb, Jack; University of New Hampshire, Earth System Research Center/EOS Heinlein, Laura; University of California Davis, Department of Land, Air and Water Resources Anastasio, Cort; University of California Davis, Department of Land, Air, and Water Resources

SCHOLARONE™
Manuscripts

Journal Name

ARTICLE TYPE

Cite this: DOI: 00.0000/xxxxxxxxxx

The interplay between snow and polluted air masses in cold urban environments

Jonas Kuhn[a], Jochen Stutz[a], Thorsten Bartels-Rausch[b], Jennie L. Thomas[c], Meeta Cesler-Maloney[d], William R. Simpson[d], Jack E. Dibb[e], Laura M. D. Heinlein[f], Cort Anastasio[f]

Received Date
Accepted Date

DOI: 00.0000/xxxxxxxxxx

The role of persistent snow covers in winter-time urban air pollution chemistry remains largely unexplored. The interaction of chemistry and transport processes are complex and the physicochemical structure of snow is uncertain. For instance, it is still unclear to what extent uptake and chemistry occur on ice, a disordered interface layer on the ice, or in brine pockets at grain boundaries. We use a process-based one-dimensional coupled atmosphere-snow model to gain initial insight into the interaction of snow with high concentrations of SO_2 and NO_2 in polluted winter-time Fairbanks, AK, USA. Snow can act as a reservoir for both gases, allowing for fluxes into the snow (during polluted periods) and out of the snow (during cleaner periods). The geometrical distribution of liquid on ice is varied to approximate the conceptual difference between the disordered ice interface and brine in localized pockets. The behavior of SO_2 is more sensitive to these differences, mostly due to its greater stickiness on ice and solubility in water compared to NO_2, which remains mostly in the snow interstitial air. Liquid phase chemical processing of both compounds is almost insensitive to the distribution of the liquid phase in the snow and mostly determined by the volume of liquid. Our study highlights the value of comprehensive process-based modeling to further our understanding of snow chemistry. Our model platform can serve as a tool to inform and support future research efforts on improving our understanding of the liquid content of snow, chemical processing on ice surfaces, and, in general, the influence of snow on atmospheric chemistry.

1 Introduction

Winter-time air pollution is a common phenomenon in many urban areas. Its negative impacts on human health are well documented with the most famous example of the Great Smog of London in December 1952[1–3]. Despite the long history of urban air pollution and related mitigation efforts, high concentrations of air pollutants such as SO_2, NO_2, and particulate matter remain a serious environmental problem today in many urban areas during winter.

High pollutant concentrations in winter cities are formed through a combination of high emissions at the surface, mostly by traffic and residential heating, stable boundary layers, which trap pollutants near the surface, and cold and low-light air chemistry[4–6]. In many cases snow is also present in these cities, where it plays an active role for the surface radiative budget influencing the dynamics of the boundary layer[7–12]. The role of snow as a sink, reservoir, and chemical reactor that can impact urban air quality and water pollution during snow-melt, has received much less attention[13–16].

Snow chemistry has mostly been discussed in the context of polar ice sheets, where trace gas concentrations are low. The processing of nitrogen and halogen species has received particular attention and it is now well established that nitric acid and NO_2 are taken up in the snow where they undergo chemical processing to be released as NO_x and HONO. Several detailed modeling studies have investigated this system confirming the relevance of snow for the recycling of deposited nitrogen and halogen species[14,17–19].

In urban areas, pollutant deposition in snow has been discussed based on snow pollutant levels[20,21]. A more detailed look at the chemistry of urban snow and its impact on the atmosphere has shown that nitrogen chemistry can lead to the formation of NO_x and HONO[22–24] and the formation of $ClNO_2$ from reaction of N_2O_5 with chloride.[25,26].

Despite the process-specific insight provided by these studies, a more comprehensive investigation of the role of snow for the

[a] Department of Atmospheric and Oceanic Sciences, University of California, Los Angeles, USA.
[b] Paul Scherrer Institute, Laboratory of Atmospheric Chemistry, Villingen, Switzerland.
[c] Université Grenoble Alpes, CNRS, Grenoble, France
[d] University of Alaska, Fairbanks, USA
[e] University of New Hampshire, Earth System Research Center/EOS, Durham, New Hampshire, USA
[f] Department of Land, Air, and Water Resources, University of California, Davis, USA

loss, release, and chemical processing of urban air pollutants is currently not available. This deficiency is in part due to a lack of well-tested parameterizations of air-snow exchange, which is believed to be a combination of molecular diffusion and wind-enhanced vertical transport[27,28]. Most recent modeling studies[29,30] rely on theoretical work by Cunningham and Waddington[31], who parameterized vertical air movements at the snow top as a function of wind speed and snow surface geometry. Only few studies have attempted to approach wind-enhanced transport in snow experimentally[32] and consequently considerable uncertainties on the magnitude of fluxes of gases in and out of snow persist.

The details of chemical and physical interactions of gases with ice grains in snow is also not well understood. Snow can include pure ice surfaces, surfaces with a disordered air-ice interface, and liquid brine, which is believed to be located at snow grain boundaries. The exact physicochemical interactions in these compartments are still under debate, with particular uncertainties on the nature and behavior of the disordered interface layer[19,33].

Finally, there is a lack of available tools that allow the quantitative assessment of the coupled chemistry-transport system that underlies air-snow interactions. Few detailed coupled air-snow models have been developed[29,30,34] and applied to individual studies of halogen and nitrogen chemistry in polar regions. Here we introduce the 'Platform for Atmospheric Chemistry and Vertical Transport in one Dimension with Snow' (PACT-1D-Snow), a new coupled atmosphere-snow model platform, that follows the experience gained in previous model developments, to better investigate the role of snow on urban air quality. Our model, for instance, allows for the implementation of different physicochemical representations of snow, to provide qualitative and quantitative insights into poorly understood chemical and physical processes in snow and their interplay with atmospheric pollutants. We simulate the combined chemistry and transport processes in snow with the aim to gain initial insight into the complex interplay between atmospheric trace gases and snow. In this work we focus on understanding the interaction of snow with high atmospheric concentrations of NO_2 and SO_2 in polluted urban environments.

We chose NO_2 and SO_2 as example compounds because, besides being some of the most abundant pollutants, both gases are very volatile but show different interactions with ice and snow. SO_2 adsorbs readily on ice and also hydrolyses effectively[35]. In contrast, NO_2 is less sticky and less prone to hydrolysis[36]. In addition, SO_2 partitions more effectively to the liquid phase as it hydrates and then dissociates into ions. This contrast allows us to to gain insight in how trace gases with different physicochemical properties behave in snow.

We apply PACT-1D-Snow to the case of Fairbanks, AK, USA, using observations during the 2022 Alaskan Layered Pollution and Chemical Analysis (ALPACA) field campaign. Fairbanks experiences strong pollution events in winter, with SO_2 and NO_x mixing ratios exceeding 30 ppb and 200 ppb in shallow surface layers[6], providing an ideal case study for this discussion.

We give a brief overview of the ALPACA experiment and the observations relevant for our study , followed by a description of PACT-1D-Snow (Section 2). The modeled NO_2 and SO_2 distributions as well as their fluxes in and out of the snow will be discussed with respect to the driving mechanisms, which include, diffusive and wind-enhanced mixing, adsorption, partitioning to brine pockets (BPs) or disordered interfaces (DIs) and the chemistry therein (Section 3).

2 Methods

2.1 The ALPACA experiment

The Alaskan Layered Pollution and Chemical Analysis (ALPACA) field campaign took place during January and February 2022 in Fairbanks, AK, USA. Improving our understanding of the physical and chemical processes in shallow polluted urban surface layers and the influence of snow were among the central goals. Simpson *et al.*[6] provide a detailed overview of ALPACA, including a description of the various observations used in this study.

By using a process-based and observation-driven model approach, we want to quantitatively assess the influence of the persistent snow layer on the atmospheric composition near the surface. We focus on the period from Jan 25 to Feb 5, 2022, which is in between two snowfall events. The period is characterized by cold temperatures, low surface winds, and heavily polluted shallow surface layers (<50 m height), which persisted for several days.

2.2 A one-dimensional, observation driven, atmosphere-snow model

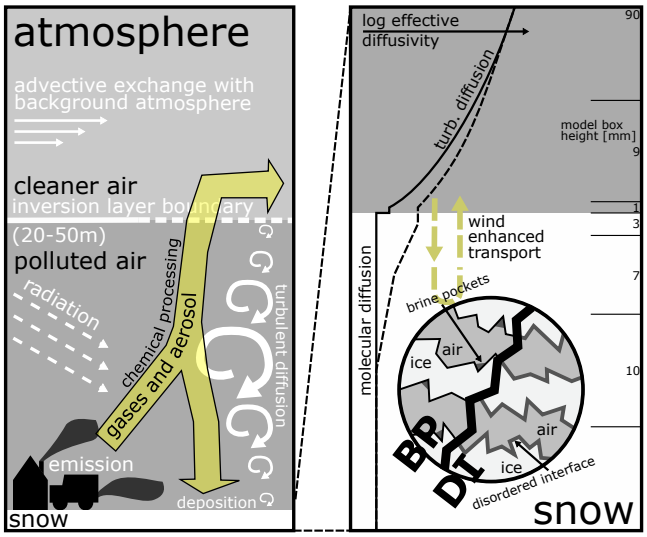

Fig. 1 Schematic of the processes included in PACT-1D-Snow for modeling of the ALPACA campaign. Emitted gases and particles experience mixing and chemical processing in the boundary layer before a fraction of it is being transported to the snow. Exchange of interstitial air with the atmosphere can be enhanced by wind, while otherwise being limited by molecular diffusion. We distinguish between two conceptual perspectives to the multiphase structure of snow: (1) solid ice surface with brine pockets (BP), (2) disordered ice interface (DI) represented by a liquid film in the model.

PACT-1D[37] was developed for the investigation of vertical trace gas distributions in Earth's atmosphere near the surface. Con-

strained by observed boundary conditions (e.g. meteorology, actinic fluxes, turbulent diffusivity, emissions), PACT-1D calculates the temporal evolution of the vertical concentrations profiles of pollutants relying on chemical kinetics. Comparing the results to measurements of trace gas distributions allows the identification and quantification of the underlying chemical and transport processes in the atmosphere[37,38].

The application of a 1D model to a confined urban area like Fairbanks is a simplification as pollutant sources are not always distributed homogeneously. However, it has been shown that atmospheric composition measurements (point-like and along km long light paths) are represented well by the model if a simple (advective) exchange with the cleaner background atmosphere is assumed (see Fig. 1)[39].

For this study we expanded PACT-1D to include kinetic multiphase chemistry and a snow layer with a continuous transition from the near-surface atmosphere to the interstitial air in snow. The extended model (PACT-1D-Snow) enables the adjustment to different representations of the snow structure and chemistry. The flexibility in the model setup and in the description of snow provides a test-bed to better understand air-snow exchange, the role of ice adsorption, and the significance of chemistry in brine pockets vs. on disordered ice-air interfaces. The following subsections describe PACT-1D-Snow in more detail and Figure 1 shows a summarizing schematic.

2.3 Gas-phase and aerosol chemistry

Investigating processes in snow critically relies on knowledge on the composition of the atmosphere above the snow, as well as multi-phase chemical processes above and in the snow. Gas-phase chemistry in PACT-1D-Snow occurs in the atmosphere as well as in the interstitial air in snow. PACT-1D-Snow uses the RACM-2 chemical mechanism[40] to simulate polluted urban air chemistry. The gas-phase mechanism is coupled to a kinetic aqueous aerosol chemistry scheme that includes basic nitrogen and sulfur processing[30,41]. Photochemistry is driven by measured photolysis frequencies.

2.4 Air-snow gas exchange

Transport of pollutants towards and away from the snow surface from the atmospheric side is driven by turbulent mixing, which is commonly assumed to vanish at the surface. However, as snow is a porous medium, horizontal air movements (wind) above the surface can penetrate the upper millimeters to centimeters of the snow layer[43]. The related vertical airflow in and out of the snow has been parameterized by Cunningham and Waddington[31], based on horizontal wind speed and the geometry of the snow surface. They are converted to effective turbulent diffusivity enhancements slightly above and below the top of the snow layer[29,30], introducing a wind dependency of the magnitude of exchange between the atmosphere and snow interstitial air (see Fig. 1). Consequently, mixing in the interstitial air in the upper millimeters to centimeters can exceed the limit otherwise set by molecular diffusion. During ALPACA this occurred when wind-

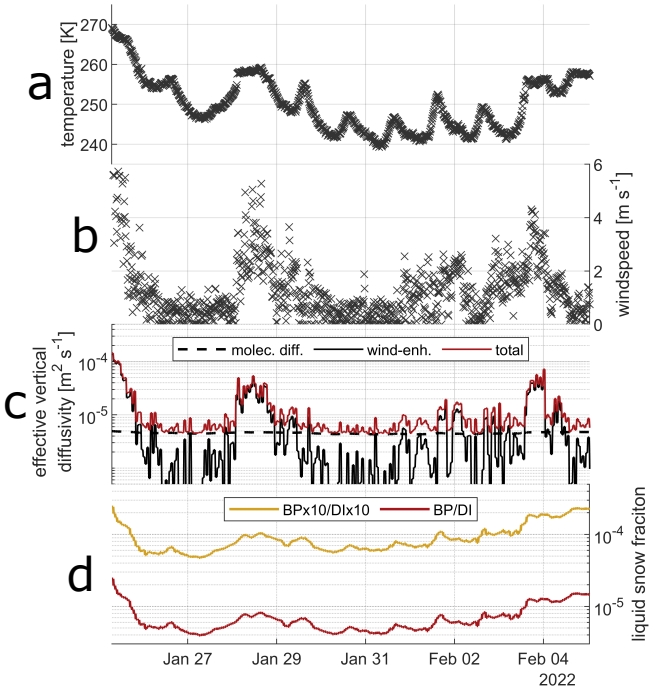

Fig. 2 (a) Temperature (3 m above ground) from January 25 to February 5, 2022, during the ALPACA experiment; (b) Wind speed measured 3 m above ground; (c) effective diffusivity at the snow-air interface, separated into molecular diffusion (dashed line), wind enhancement calcualted from the wins speed in (b)(solid black line) and the sum of the two components (red line). Higher wind speeds enhance mixing during clean and less stable periods. (d) Liquid snow fraction calculated according to the parameterization of Cho *et al.*[42](BP/DI, red curve). The yellow curve shows the liquid snow fraction enhanced by a factor of 10 as used in the BPx10/DIx10 model runs.

speeds exceeded 1 m/s (Fig. 2c). Periods with higher wind speeds and enhanced atmosphere-snow exchange were associated with less polluted conditions, while strong surface inversions with high pollutant levels were characterized by low wind speeds. In our model, gases can freely exchange between interstitial air and the atmosphere. Aerosol particles are assumed to be deposited after reaching the snow top via turbulent transport, adding their constituents to the snow chemical composition.

In order to accurately represent air-snow gas exchange and its interaction with chemical processes, the vertical grid spacing decreases in both directions from the snow surface (see Fig. 1). Moreover, the time step of the sequential solving approach of the transport and chemistry parts of the differential equation system (operator splitting) is adapted to the characteristic mixing time ($\frac{\Delta z^2}{2K_{eff}}$; Δz: box height, K_{eff}: effective diffusivity) of the individual model boxes.

2.5 Physicochemical processes in snow

In our model snow consists of three compartments: interstitial air (gas-phase), solid ice, and a liquid phase. Snow interstitial air is in direct contact with the solid and liquid snow surface, and interacts via the kinetics of liquid phase uptake and adsorption/desorption of trace gases to the solid ice surface. We implemented the kinetics of adsorption of gas molecules to the ice

Table 1 Properties of snow

property	BP (BPx10)	DI (DIx10)
snow density	100 kg m^{-3}	
specific surface area[44]	80 m^2 kg^{-1}	
tortuosity	1.33	
liquid volume fraction (250 K)	$3 \cdot 10^{-5}$ ($3 \cdot 10^{-4}$)	$3 \cdot 10^{-5}$ ($3 \cdot 10^{-4}$)
liquid surface fraction (250 K)	$3 \cdot 10^{-5}$	1
adsorbing ice surface fraction	≈ 1	0

surface, balanced by a release/desorption process, which ensures that the equilibrium, if reached, is approximated by the linearized Langmuir formalism[45].

Details on the presence of a liquid phase in cold snow remain under debate. Liquid might be present in snow as brine pockets (BPs), whose formation is determined by the melting point depression of salt components in snow. The liquid phase might, however, also be explained by the disordered interface (DI) of ice. The DI refers to the premelting at the air-ice surface. It is the result of the increasing number of motion-related degrees of freedom of hydrogen-bonding network compared to that of interior crystalline ice. Treating the DI as a liquid film, as in this work, might represent a rather coarse approximation of reality. The liquid fraction of the snow volume (associated with both BPs and the DI) is calculated based on temperature and snow ion content according to the parametrization of Cho *et al.*[42]. Snow geometry is based on snow density measurements during ALPACA and a corresponding specific surface area of freshly fallen snow (see Tab. 1)[44].

The geometrical distribution of the snow liquid fraction can be adjusted in the model. In this study, we consider four configurations, covering the two extremes of all liquid water in BP vs. ice covered with a liquid film representing the DI. The behavior of mixed states, that is snow in which BPs and DIs exist simultaneously, is expected to lay between the two end-member cases. We also investigate the influence of an increase of the total amount of liquid/brine in snow by a factor of 10. The resulting four cases are as follows (see also Tab. 1):

- **BP case:** For the BP case we assume that snow consists of a combination of a solid ice surface and brine pockets. The amount of brine is calculated via the parametrization from[42] for the ALPACA temperatures (Fig. 2a) and snow ion concentrations. The liquid snow fraction varies between 3×10^{-6} and 2×10^{-5}, with the smallest values associated with the lowest temperatures (Fig. 2d). Liquid phase chemistry occurs in the brine pockets, while at the ice surface, which is much larger than the surface of the brine pockets, adsorption/desorption processes dominate.

- **BPx10 case:** To understand the impact of brine volume we increased the volume of liquid by a factor of 10 compared to the BP case (Fig. 2d), reflecting the upper limit reported by[42] for ocean water. All other parameters as well as chemistry are identical to the BP case.

- **DI case:** In the DI case we assume that the ice is covered with a DI with a volume equivalent to the brine pockets in the BP case (Fig. 2d). The same chemical mechanism is used, however there is no solid ice surface and, thus, no adsorption/desorption.

- **DIx10 case:** Equivalent to the BIx10 case, the DIx10 case is identical to the DI case, except for an increase of the liquid volume by a factor of 10.

3 Results and Discussion

3.1 Atmospheric Transport and Chemistry

The performance of PACT-1D-Snow was investigated by comparing field observations of vertical trace gas profiles from long-path differential optical absorption spectroscopy (LP-DOAS) instrument and surface in-situ observations[6]. Here we show the LP-DOAS measurements along a 1154 m long light path between the main instrument, which was located in a parking garage in downtown Fairbanks at 17 m agl, and a reflector array located on a roof east of the garage at 11.5 m agl. Measurements on this path were preformed approximately every 30 min. Data analysis was performed using the DOAS method[46] and literature absorption cross sections of SO_2[47] and NO_2[48] in the 292 - 312 nm and 345 - 371 nm wavelength range. It is beyond the scope of this work to provide a full discussion of these efforts. We will focus on the performance of the model for SO_2 and NO_2 in the surface layer. For the time period discussed here, PACT-1D-Snow agrees well with observations in the 11.5 - 17m altitude interval. Specifically, it reproduces the variation between a stable surface layer and high mixing ratios of both species during Jan 26 - Jan 28 and Jan 30 - Feb 3, 2022, and periods with stronger vertical mixing and lower mixing ratios on Jan 28, and during the night from Feb 3 to 4, 2022 (Fig 3).

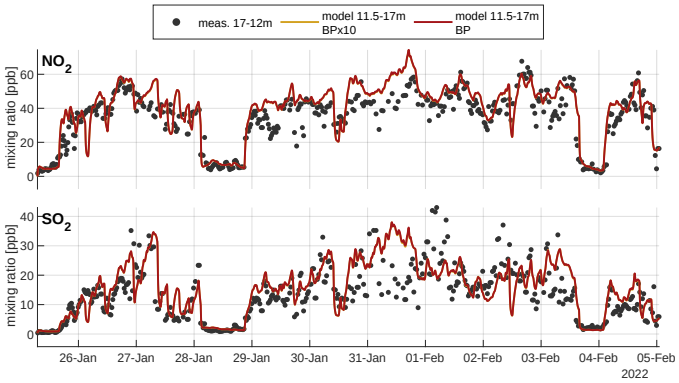

Fig. 3 Comparison of observed NO_2 and SO_2 mixing ratios at 12 - 17 m above ground with output for two model cases, BP and BPx10. The results of both model runs overlap indicating negligible effect of the snow liquid fraction to the enhanced atmospheric concentrations of NO_2 and SO_2 aloft. Typical measurement errors for SO_2 and NO_2 are 0.15ppb and 0.25ppb, respectively.

The excellent performance of PACT-1D-Snow in the surface layer gives us confidence that the near-surface atmospheric

mixing as well as trace gas levels are reflected well in the model. While not shown here, this is further supported by PACT-1D-Snow also reproducing observations of vertical profiles between 11.5 and 200 m altitude in Fairbanks. We can therefore analyze the impact of pollution events on snow composition by zooming into the lowest 0.5 m of the atmosphere above the snow and the top 0.5 m of the snow layer. The atmospheric mixing ratios of NO_2 (Fig. 4) and SO_2 (Fig. 5), right above the snow follow the trend already shown in Figure 3 with variations between high mixing ratios (dark shading) and low mixing ratios (light shading).

3.2 The distribution of SO_2 and NO_2 in snow interstitial air

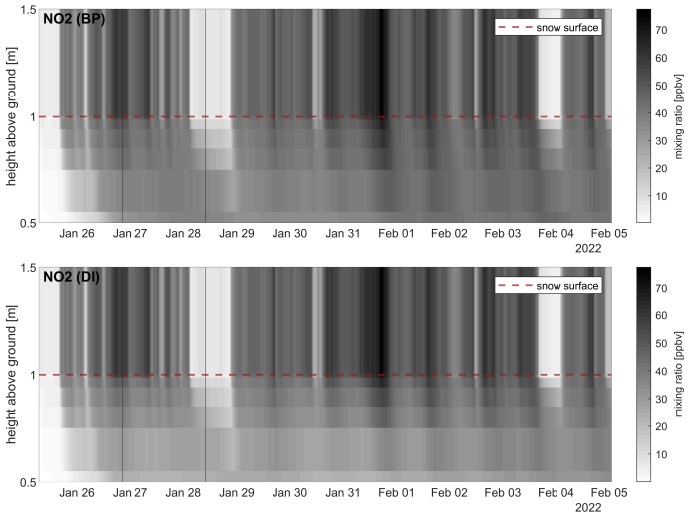

Fig. 4 NO_2 mixing ratios simulated by PACT-1D-Snow in the lowest 0.5 m above the snow and in interstitial air down to 0.5 m depth from Jan 25 - Feb 5, 2022. The red dashed line denotes the snow surface at 1 m. The detailed vertical profiles for the times indicated by the vertical lines are shown in Fig. 7.

In the BP case interstitial NO_2 roughly follows the atmospheric mixing ratio at the snow top (Fig. 4). NO_2 is mixed below 0.5 m depth even during calm polluted periods. There is an apparent tilt in the spatio-temporal distribution of NO_2 that reflects the transport process and its time scale. At large atmospheric mixing ratios there is a negative gradient in the mixing ratio of NO_2 in the snow interstitial air (more on the top of the snow than further in the snow). During the cleaner mixing events this gradient reverses and there is less NO_2 at the snow surface than below. Assuming a DI instead of BPs does not introduce significant differences to this picture.

The behavior of SO_2 is different from that of NO_2 in that SO_2 mixing ratios in interstitial air are generally lower and do not follow the atmospheric SO_2 mixing ratios as closely. SO_2 is also not mixed as deeply into the snow, only reaching depths of around 0.2 m after several days (Fig. 5). Mixing ratio gradients are generally negative and much steeper. Positive gradients during clean periods are only present right at the snow top. In the DI case SO_2 penetrates further into the snow than in the BP case

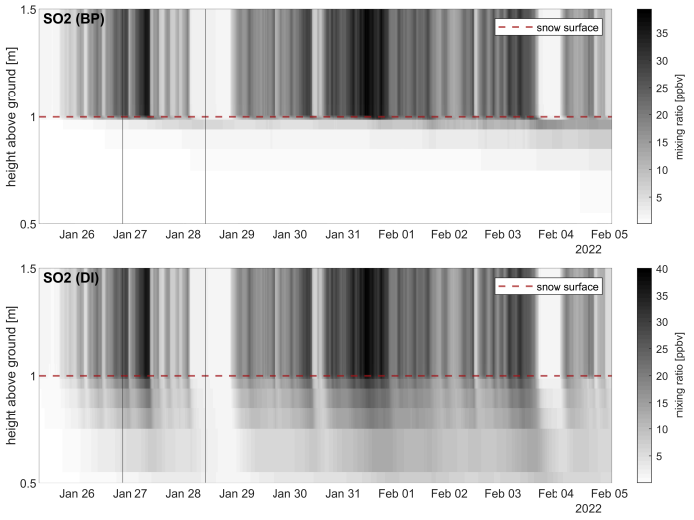

Fig. 5 SO_2 mixing ratios simulated by PACT-1D-Snow in the lowest 0.5 m above the snow and in interstitial air down to 0.5 m depth during from Jan 25 - Feb 5, 2022. The red dashed line denotes the snow surface at 1 m. The detailed vertical profiles for the times indicated by the vertical lines are shown in Fig. 7.

(Fig. 5). Interstitial SO_2 also follows atmospheric mixing ratios more closely than in the BP case. The different behavior of SO_2 and NO_2 in the snow interstitial air can be largely explained by their different partitioning onto the ice surface and to the liquid phase. The ice surface adsorption-desorption distribution coefficient (linear Langmuir coefficient) at 250 K is 2.8 cm for SO_2 and only 1.2×10^{-4} cm for NO_2, with a temperature dependence that is negligible for the conditions considered in this work[45]. Consequently, most SO_2 'sticks' to ice surfaces, while NO_2 distributes more homogeneously throughout the snow interstitial air. Even for the DI cases, SO_2 is transported slower into the snowpack than NO_2. This is due its higher effective solubility, which will be discussed below.

Our model results show that snow is closely linked to the overlaying polluted urban atmosphere. This is true for 'sticky' species such as SO_2 as well as species that interact less efficiently with ice or liquid in the snow, such as NO_2. While previous studies have shown that NO_2 can penetrate deeply into the snow[30,49,50], we are not aware of previous snow-atmosphere modeling studies of SO_2.

3.3 Trace gas fluxes in and out of the snowpack

To further investigate the role of snow we look at the modeled gas fluxes in and out of the snow. Figure 6 shows the instantaneous flux density through the top of the snow layer (positive is the flux from snow to the atmosphere) and the cumulative net flux starting from the beginning of the modeled period. Chemical conversion rates, plotted in dashed lines, will be discussed below. The cumulative net NO_2 flux can become negative if the flux of NO_2 out of the snow becomes larger than the flux into the snow for an extended period. This happens, for example, due to the flux of ozone and NO into the snow followed by the chemical formation of NO_2 in interstitial air. When the newly formed NO_2

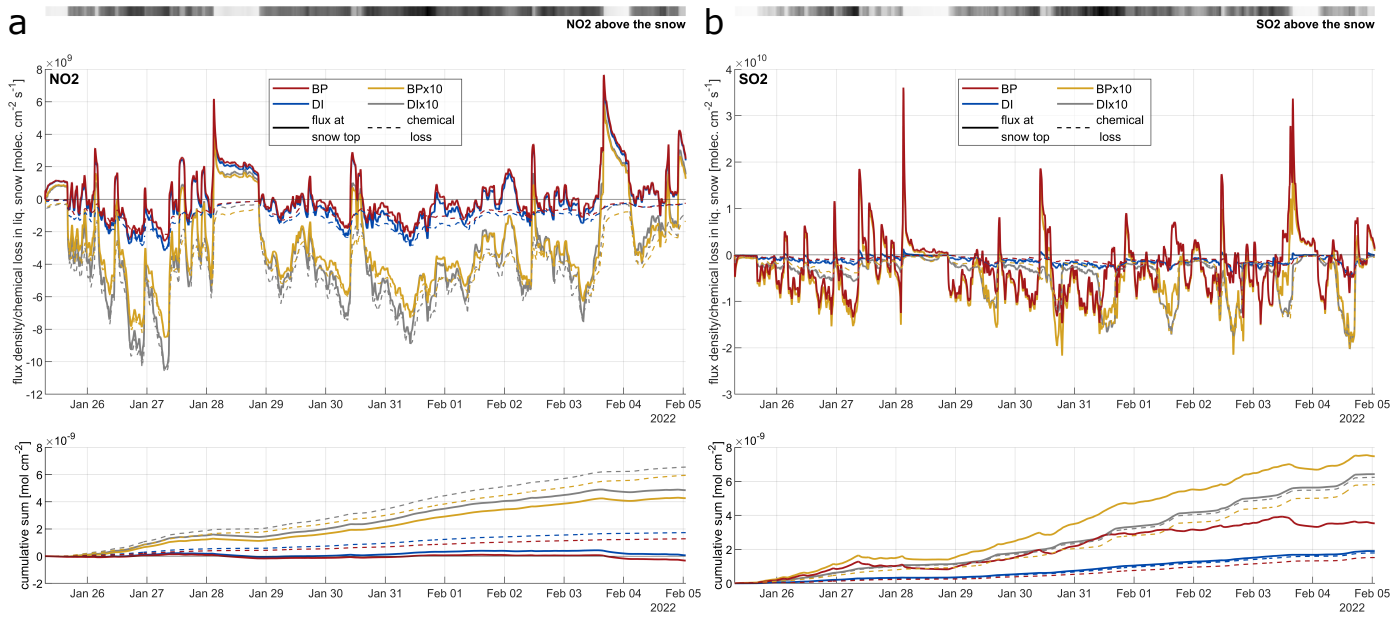

Fig. 6 Comparison of fluxes through the atmosphere-snow interface (solid lines) and vertically integrated chemical loss rates (dashed lines) in the snow for NO_2 (a) and SO_2 (b) and all four model runs. Positive values represent fluxes out of the snow and negative fluxes are into the snow. Chemical loss rates are shown as negative values for better comparison with the fluxes.

leaves the snow it can increase the positive flux beyond the downward flux (e.g. at the beginning of the period). This shows that the fluxes as well as the cumulative value needs to be interpreted with care due to the chemistry in the snow-pack.

In the BP model run there is a clear net flux into the snow for high atmospheric NO_2 mixing ratios, while the flux is out of the snow whenever atmospheric mixing ratios are low. When increasing the snow liquid fraction by a factor of 10 (BPx10) we see a similar temporal behavior than in the BP case, but the fluxes are generally more negative, i.e. the flux into the snow outweighs the flux out of the snow. This is also reflected in the cumulative net flux of NO_2 (Fig. 6), which shows that there is considerably more deposition in snow. This suggests that liquid-phase chemistry drives deposition, as will be discussed below in more detail.

SO_2 fluxes in the BP case can also be both negative and positive. As in the case of NO_2, SO_2 comes out of the snow during clean periods. However, SO_2 shows much more pronounced peaks in the SO_2 outward fluxes during the polluted-clean transition and near zero fluxes later during a clean air event. This is largely because SO_2 is located predominantly at the top of the snow layer, which is influenced by surface winds and, thus, mixes effectively with the atmosphere. It should be noted here that high atmospheric mixing ratios are often associated with low surface wind speeds and thus slow and inefficient mixing between atmosphere and snow, while wind speeds are enhanced during clean periods. A few centimeters inside the snow, where molecular diffusion dominates transport, the release of adsorbed and dissolved SO_2 is limited by molecular diffusion, which only leads to marginal decreases of interstitial SO_2 during clean events in the BP case (see Fig. 5). When parameterizing uptake to the ice surface by partitioning to the liquid film in the DI cases, less SO_2 accumulates in the snow. Moreover, fluxes are far less variable and the smaller total amount of SO_2 present in the snow is able to leave the snow quickly during clean periods.

Compared to the urban emission sources, responsible for the high amounts of SO_2 and NO_2, the fluxes in and out of the snowpack are typically on the order of 1%. However, for the BP cases, peak SO_2 fluxes at the break down of the surface inversion (transition between polluted and clean atmospheric conditions) can reach up to 10% of the typical urban emissions close to the surface.

3.4 Budgets and the role of the different snow compartments

Our model includes representation of three different compartments for trace compounds: gas phase, liquid phase, and the ice surface. Each of the compartments allows for different physical and chemical processes to occur. It is thus instructive to investigate how SO_2 and NO_2, are distributed among these compartments and how this impacts the role snow plays as a reservoir for pollutants. It should be noted here that we do not explicitly treat the SO_2 hydrolysis when adsorbed on solid ice but assume that it keeps its molecular structure. The effective adsorption coefficient includes hydration at the ice surface. In the liquid phase we account for the explicit ionization of dissolved SO_2. As this is a reversible process, we will regard $S(IV) = SO_2 \cdot H_2O + HSO_3^- + SO_3^{2-}$ as the effectively dissolved amount of SO_2. In the case of NO_2, which does not ionize, the liquid phase species is dissolved NO_2.

Figure 7 combines the vertical profiles of SO_2 and NO_2 in the different snow compartments for the four snow implementations. We distinguish a case with a polluted surface layer and a clean case, to illustrate how the overlying atmosphere impacts the vertical distribution of the two pollutants in the snow.

For the BP case, with only small amounts of liquid water, ice

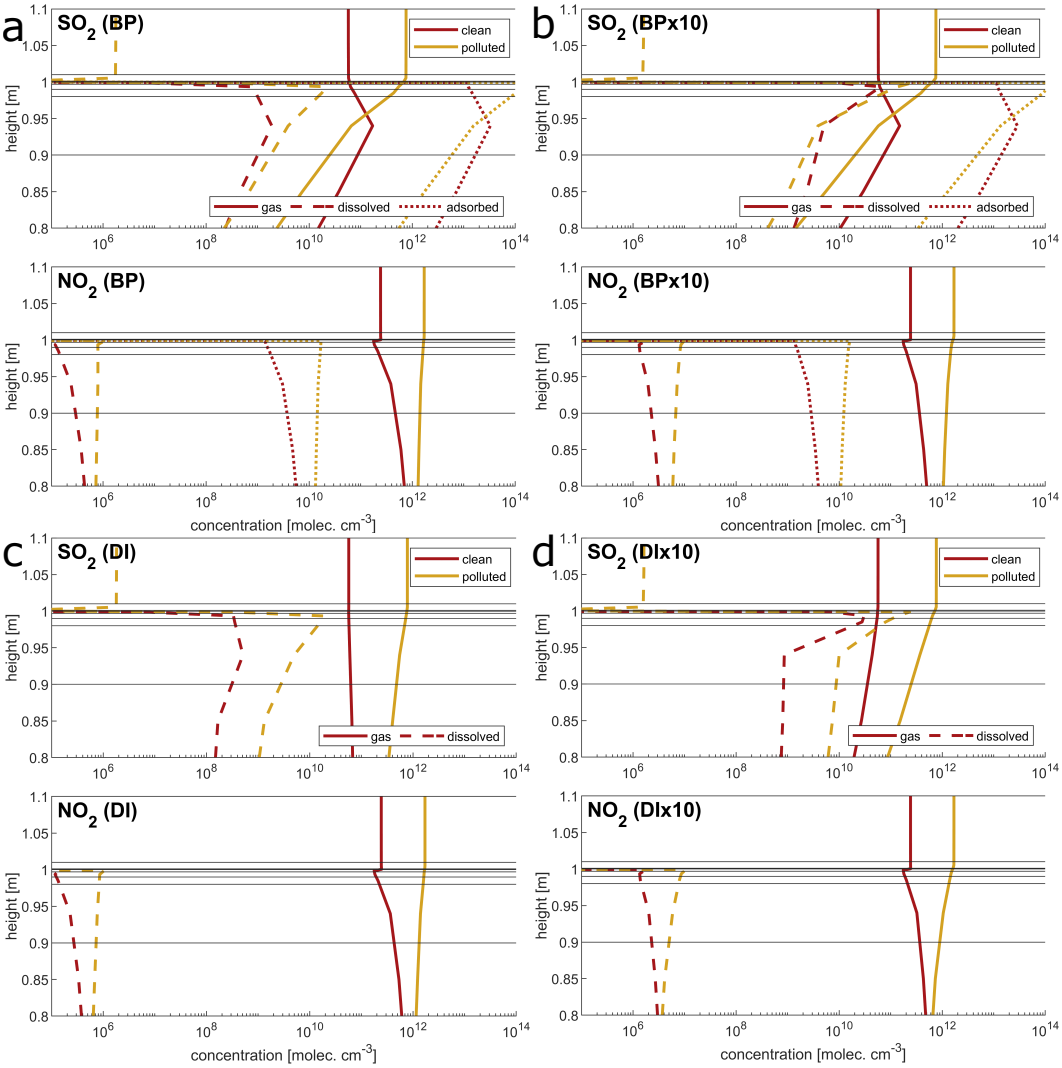

Fig. 7 Concentration of SO_2 and NO_2 in the different phases (gas, dissolved in liquid, adsorbed at ice surface) at the snow-atmosphere interface (at 1 m height) for a polluted shallow surface layer scenario and a cleaner unstable scenario (vertical lines in Fig. 4 and 5 indicate the times of the shown profiles)

adsorption dominates for SO_2, at all depth in the snow, while most of NO_2 is in the gas-phase in interstitial air. In both cases the liquid phase is the least prominent compartment. Increasing the liquid water content in the BPx10 case increases the amount of dissolved molecules the liquid phase almost linearly. This introduces a small reduction in the other two compartments.

As already observed in Fig. 5, the vertical profiles of the sulfur species show a steep decrease with depth, which is associated with fast adsorption of SO_2 onto the ice surface and partitioning into the liquid phase during downward transport. After the transition to a cleaner atmosphere, in the BP case, gradients of sulfur in all compartments become negative in the top 5 cm, in agreement with the modeled positive fluxes out of the snow. While adsorbed SO_2 remains in equilibrium with the gas phase, the dissolved S(IV) reacts slower to changes in the SO_2 concentration in the interstitial air. This becomes more clear in the BPx10 case with increased snow liquid fraction. Sulfur profiles below 5 cm change little, mostly because transport from deeper depths to the top of the snow is limited by molecular diffusion and adsorption and thus much slower.

In the BP cases, almost all the SO_2 that enters the snow is adsorbed at the ice surfaces (more than two orders of magnitude more than in other compartments). This means for instance that, in order to balance an atmospheric concentration change in the snow interstitial air at the snow top about 100 times the number of SO_2 molecules need to enter/leave the snow. This effect explains the considerably higher SO_2 fluxes into and out of the snow in the BP case as compared to the DI cases, where no adsorption is assumed.

Because NO_2 is much less soluble and sticky, it distributes more homogeneously in the snow volume. NO_2 remains predominantly in the gas-phase and, thus, is more effectively transported downward in the snow. Clean periods again induce a negative but less steep concentration gradients reflecting the flux of NO_2 in the interstitial air out of the snow. The amount and distribution of the snow liquid phase only marginally affects the profiles of NO_2.

3.5 The role of chemistry in BPs and DI

To further disentangle the fate of NO_2 and SO_2 molecules which have entered the snow, we analyze the amount of chemical processing of both species in the BPs and the DI. In our model, we describe the chemical processing in both the BPs and the DI cases with the same aqueous phase chemical mechanism. It should be reiterated that the differences are predominantly due to the way the hypothetical liquid is distributed on the snow/ice surface. That is to say, the DI cases expose a much larger liquid surface area to the interstitial air than the BP cases in an approach to mimic/reproduce the conceptually different physical representations of snow.

We will not discuss the details of the precise chemistry here and just focus on the analysis of the total rate of irreversible S(IV) and NO_2 chemical processing, integrated over the entire snowpack. While we expect distinct depth dependence of the chemistry, the choice of integrating the rates over entire snow depth allows a better comparison to the net deposition fluxes. For a detailed discussion of the chemical processes occurring in the snow we refer to forthcoming publications.

Figure 6 shows the chemical loss rates integrated over the snowpack (dashed lines) alongside with the above discussed trace gas fluxes into and out of the snow. Moreover the cumulative chemical loss is calculated. For both NO_2 and SO_2, we find that chemical processing is much more dependent on the volume of BPs and the DI (i.e. the assumed liquid fraction of the snow) than on the exposed liquid surface area. For both gases chemical loss is enhanced in the DI cases, however, by an amount that is small considering the increase in surface to volume ratio by more than 3 orders of magnitude. The small sensitivity to the liquid surface to volume ratio indicates that interstitial gas and snow liquid phase equilibrate quickly in the BP case. That is to say that in both the BP and DI cases, the mass transfer aspects of the uptake do not significantly limit liquid phase chemical processing. Chemical loss increases significantly when increasing the total BP and DI volume. The apparent non-linearity in this relation (the loss rates do not strictly increase by the factor of 10 by which the liquid fraction increases) is mostly due to changing influences of aerosol deposition and the vertical inhomogeneity, which we will not further discuss here.

A comparison of total snow chemical loss of NO_2 and the flux into the snow from the atmosphere reveals that in all model cases irreversible chemical conversion in BPs and DIs drives the flux of NO_2 into the snowpack. Chemical conversion tends to be always slightly higher than the inward fluxes. This is due to the chemical conversion or outward flux of NO_2, which was formed in the snow interstitial air, mostly from ozone and NO. Because ozone has very low concentrations under polluted conditions this effect is most prominent during clean periods. Consequently, when assuming low liquid fractions in the BP and DI model runs, the cumulative net flux of NO_2 into the snow almost vanishes throughout the modeled period.

SO_2 fluxes into the snow are always larger than chemical conversion rates in the BPs and the DI. In the DI cases, where no ice adsorption is assumed, chemical loss clearly drives the SO_2 flux into the snow. While chemical processing in the BP cases is similar to that in the DI, it is superimposed by much higher trace gas fluxes driven by the interplay of the large reservoir of adsorbed SO_2 with atmospheric variation.

Overall we can conclude that chemical processing in BPs or the DI are responsible for driving the longer-term net flux/deposition of NO_2 and SO_2 into the snow. At the beginning of the modeled period, the dominant reaction for the NO_2 and SO_2 loss is the reaction of S(IV) species with two NO_2 molecules in the liquid phase[32]. As chemical processing and aerosol deposition gradually acidifies the snow pH independent processes, such as NO_2 hydrolysis[51], and sulfate production from the photolytically produced hydrogen peroxide[52] take over. Forthcoming comparison with snow composition measurements might reveal chemical conversion pathways, which are specific to the heavily polluted environments studied here and not yet accounted for by the present liquid phase chemical mechanism (e.g. the influence of Fenton-type reactions in polluted snow). These might further enhance the net chemical conversion rates.

As expected from the above discussed transport processes, chemical processing is much weaker during clean periods, as pollutant concentrations in the interstitial air adapt to atmospheric concentrations within hours. This also leads to a depletion of dissolved NO_2 and SO_2 in snow (with the exception of SO_2 in the BP case). The driving chemical processes in snow considered in our model are not sensitive to differences in the geometrical distribution of the pseudo-liquid phase in the BP and DI cases. Chemical processing rates are mostly controlled by the liquid fraction of the snow and can be influenced by snow composition changes through aerosol deposition. This indicates a highly complex system behind deposition processes of gaseous pollutants in snow in these polluted environments.

Conclusions

Many urban areas experience a persistent snow cover in winter. The impact of surface snow on urban air quality is currently poorly understood. To provide initial quantitative insight into this question we focus on understanding how two of the most important wintertime pollutants, SO_2 and NO_2, interact with snow. We simulated a pollution episode in Fairbanks, AK, USA, with a new one-dimensional coupled atmosphere-snow model. PACT-1D-Snow shows that SO_2 and NO_2 are efficiently transported into the snow through a combination of molecular diffusion and wind-induced enhancements of vertical transport at the snow top. The same processes can also lead to transport of pollutants out of the snow during times when the atmospheric concentrations fall below those in snow interstitial air. This reservoir behavior of snow depends on the trace gas solubility and stickiness to ice surfaces and is thus different for SO_2 and NO_2.

For SO_2, the reservoir behavior of snow is sensitive to the distribution of the liquid phase in the snow. When assuming that the snow surface is mostly solid ice with brine pockets at grain boundaries, reversible adsorption at the ice surface leads to high

concentrations of SO_2 close to the top of the snow layer. This causes fast and pronounced responses to concentration changes in the atmosphere. In the case of NO_2, which tends to adsorb less on ice surfaces and is less soluble than SO_2, the dominant compartment is the snow interstitial air. This means that NO_2 is distributed more homogeneously throughout the snow volume and outward fluxes become limited by molecular diffusion once the interstitial air at the snow top, where mixing is influenced by wind, has adapted to atmospheric concentrations.

When the amount of water in the brine pockets or disordered interface is increased, chemical processing becomes more important. While the bidirectional fluxes still occur, the downward flux – enhanced by the chemical loss – now dominates. Long-term net fluxes of NO_2 and SO_2 into the snow are driven by irreversible chemical conversion in the BPs or DIs (treated as a liquid in the model). The chemical processing of SO_2 and NO_2 in the liquid compartments is not very sensitive to the geometrical distribution of the assumed liquid phase on the snow surface. That is to say, chemical loss – eventually driving deposition – is mainly controlled by the amount of liquid in snow.

Our results highlight how the complex nature of snow can impact the behavior of NO_2 and SO_2 in a snowy atmosphere. Despite using a simplified physicochemical representation of snow, our approach allows basic quantitative insights into the interplay between snow and polluted air masses. Our model identified the total amount of liquid in snow as the main factor driving deposition. The geometrical distribution of liquid in snow, on the other hand, had only a minor impact.

Fundamental physicochemical processes in snow remain uncertain and more work is needed to better quantify the liquid fraction of snow under different environmental conditions and to understand the chemical processing of adsorbed and dissolved pollutants. PACT-1D-Snow provides a platform to test field and laboratory observations against current theories. Comparison of snow composition measurements to PACT-1D-Snow simulations can provide further constraints on the snow structure and snow and help design and interpret future experiments. This study highlights the complexity of the interplay of gaseous pollutant with snow. It demonstrates how process-based modeling can help to improve our conceptual and quantitative understanding of the influence of snow on atmospheri and eventually guide the development of parametrizations for regional or global air quality models.

Author contributions

Conceptualization: J.K., J.S., T.B.-R.; Methodology: J.K., J.S., T.B.-R, J.L.T., M.C.-M., W.R.S., J.E.D., L.M.D.H, C.A. ; Software: J.K., J.S., T.B.-R., J.L.T., L.M.D.H ; Visualization: J.K.; Resources: M.C.-M., W.R.S., J.E.D.; Writing - original draft: J.K., J.S. ; Writing - review & editing: T.B.-R., J.L.T., M.C.-M., W.R.S., J.E.D., L.M.D.H, C.A. ; Funding acquisition: J.S., W.R.S., J.E.D., C.A.

Conflicts of interest

There are no conflicts to declare.

Data availability

Gas and meteorological measurements during the ALPACA-2022 field study is available at the Arctic Data Center. doi:10.18739/A27D2Q87WALPACA. LP-DOAS data is available at: https://osf.io/w6pxu.

Acknowledgements

We thank University of Alaska Fairbanks and the Geophysical Institute for logistical support during ALPACA, and we thank Fairbanks for welcoming and engaging with our research. J.K. and J.S. acknowledge funding support from NSF grants 1927936 and 2109240. W.R.S. and M.C.-M. acknowledge support from NSF grants NNA-1927750 and AGS-2109134. J.L.T. is funded by the European Union's Horizon 2020 research and innovation programme under grant agreement No. 101003826 via project CRiceS (Climate Relevant interactions and feedbacks: the key role of sea ice and Snow in the polar and global climate system). J.E.D. acknowledges support from NSF grant AGS-2109023. L.M.D.H and C.A. acknowledge support from NSF grant AGS-2109011. T.B.-R. acknowledges funding by SNF (grant IZSEZ0_210264).

Notes and references

1 M. L. Bell and D. L. Davis, *Environmental Health Perspectives*, 2001, **109**, 389–394.

2 D. Laskin, *Weatherwise*, 2006, **59**, 42–45.

3 E. Wilkins, *Journal of the Royal Sanitary Institute*, 1954, **74**, 1–21.

4 N. P. Lareau, E. Crosman, C. D. Whiteman, J. D. Horel, S. W. Hoch, W. O. Brown and T. W. Horst, *Bulletin of the American Meteorological Society*, 2013, **94**, 51–63.

5 J. Schmale, S. R. Arnold, K. S. Law, T. Thorp, S. Anenberg, W. R. Simpson, J. Mao and K. A. Pratt, *Earth's Future*, 2018, **6**, 1385–1412.

6 W. R. Simpson, J. Mao, G. J. Fochesatto, K. S. Law, P. F. DeCarlo, J. Schmale, K. A. Pratt, S. R. Arnold, J. Stutz, J. E. Dibb, J. M. Creamean, R. J. Weber, B. J. Williams, B. Alexander, L. Hu, R. J. Yokelson, M. Shiraiwa, S. Decesari, C. Anastasio, B. D'Anna, R. C. Gilliam, A. Nenes, J. M. St. Clair, B. Trost, J. H. Flynn, J. Savarino, L. D. Conner, N. Kettle, K. M. Heeringa, S. Albertin, A. Baccarini, B. Barret, M. A. Battaglia, S. Bekki, T. Brado, N. Brett, D. Brus, J. R. Campbell, M. Cesler-Maloney, S. Cooperdock, K. Cysneiros de Carvalho, H. Delbarre, P. J. DeMott, C. J. Dennehy, E. Dieudonné, K. K. Dingilian, A. Donateo, K. M. Doulgeris, K. C. Edwards, K. Fahey, T. Fang, F. Guo, L. M. D. Heinlein, A. L. Holen, D. Huff, A. Ijaz, S. Johnson, S. Kapur, D. T. Ketcherside, E. Levin, E. Lill, A. R. Moon, T. Onishi, G. Pappaccogli, R. Perkins, R. Pohorsky, J.-C. Raut, F. Ravetta, T. Roberts, E. S. Robinson, F. Scoto, V. Selimovic, M. O. Sunday, B. Temime-Roussel, X. Tian, J. Wu and Y. Yang, *Environmental Science & Technology Air*, 2024, **1**, 200–222.

7 P. S. Anderson and W. D. Neff, *Atmospheric Chemistry and Physics*, 2008, **8**, 3563–3582.

8 H. a. M. Sterk, G. J. Steeneveld and A. a. M. Holtslag, *Journal of Geophysical Research: Atmospheres*, 2013, **118**, 1199–1217.

9 H. Savijärvi, *Quarterly Journal of the Royal Meteorological Society*, 2014, **140**, 1121–1128.

10 H. N. Q. Tran and N. Mölders, *Atmospheric Research*, 2011, **99**, 39–49.

11 C. D. Whiteman, S. W. Hoch, J. D. Horel and A. Charland, *Atmospheric Environment*, 2014, **94**, 742–753.

12 C. S. Foster, E. T. Crosman and J. D. Horel, *Boundary-Layer Meteorology*, 2017, **164**, 63–87.

13 P. A. Ariya, A. Dastoor, Y. Nazarenko and M. Amyot, *Atmospheric Environment*, 2018, **186**, 266–268.

14 J. L. Thomas, J. Stutz, M. M. Frey, T. Bartels-Rausch, K. Altieri, F. Baladima, J. Browse, M. Dall'Osto, L. Marelle, J. Mouginot, J. G. Murphy, D. Nomura, K. A. Pratt, M. D. Willis, P. Zieger, J. Abbatt, T. A. Douglas, M. C. Facchini, J. France, A. E. Jones, K. Kim, P. A. Matrai, V. F. McNeill, A. Saiz-Lopez, P. Shepson, N. Steiner, K. S. Law, S. R. Arnold, B. Delille, J. Schmale, J. E. Sonke, A. Dommergue, D. Voisin, M. L. Melamed and J. Gier, *Elem Sci Anth*, 2019, **7**, 58.

15 M. Viklander, *Science of The Total Environment*, 1996, **189–190**, 379–384.

16 H. Zhu, Y. Xu, B. Yan and J. Guan, *International Journal of Environmental Research and Public Health*, 2012, **9**, 4333–4345.

17 F. Dominé and P. B. Shepson, *Science*, 2002, **297**, 1506–1510.

18 A. M. Grannas, A. E. Jones, J. Dibb, M. Ammann, C. Anastasio, H. J. Beine, M. Bergin, J. Bottenheim, C. S. Boxe, G. Carver, G. Chen, J. H. Crawford, F. Dominé, M. M. Frey, M. I. Guzmán, D. E. Heard, D. Helmig, M. R. Hoffmann, R. E. Honrath, L. G. Huey, M. Hutterli, H. W. Jacobi, P. Klán, B. Lefer, J. McConnell, J. Plane, R. Sander, J. Savarino, P. B. Shepson, W. R. Simpson, J. R. Sodeau, R. von Glasow, R. Weller, E. W. Wolff and T. Zhu, *Atmospheric Chemistry and Physics*, 2007, **7**, 4329–4373.

19 T. Bartels-Rausch, H.-W. Jacobi, T. F. Kahan, J. L. Thomas, E. S. Thomson, J. P. D. Abbatt, M. Ammann, J. R. Blackford, H. Bluhm, C. Boxe, F. Domine, M. M. Frey, I. Gladich, M. I. Guzmán, D. Heger, Th. Huthwelker, P. Klán, W. F. Kuhs, M. H. Kuo, S. Maus, S. G. Moussa, V. F. McNeill, J. T. Newberg, J. B. C. Pettersson, M. Roeselová and J. R. Sodeau, *Atmospheric Chemistry and Physics*, 2014, **14**, 1587–1633.

20 K. Kuoppamäki, H. Setälä, A.-L. Rantalainen and D. J. Kotze, *Environmental Pollution*, 2014, **195**, 56–63.

21 Y. Nazarenko, S. Fournier, U. Kurien, R. B. Rangel-Alvarado, O. Nepotchatykh, P. Seers and P. A. Ariya, *Environmental Pollution*, 2017, **223**, 665–675.

22 V. Michoud, J.-F. Doussin, A. Colomb, C. Afif, A. Borbon, M. Camredon, B. Aumont, M. Legrand and M. Beekmann, *Atmospheric Environment*, 2015, **116**, 155–158.

23 M. Zatko, J. Erbland, J. Savarino, L. Geng, L. Easley, A. Schauer, T. Bates, P. K. Quinn, B. Light, D. Morison, H. D. Osthoff, S. Lyman, W. Neff, B. Yuan and B. Alexander, *Atmospheric Chemistry and Physics*, 2016, **16**, 13837–13851.

24 Q. Chen, J. Edebeli, S. M. McNamara, K. D. Kulju, N. W. May, S. B. Bertman, S. Thanekar, J. D. Fuentes and K. A. Pratt, *ACS Earth and Space Chemistry*, 2019, **3**, 811–822.

25 S. M. McNamara, Q. Chen, J. Edebeli, K. D. Kulju, J. Mumpfield, J. D. Fuentes, S. B. Bertman and K. A. Pratt, *ACS Earth and Space Chemistry*, 2021, **5**, 1020–1031.

26 S. Wang, S. M. McNamara, K. R. Kolesar, N. W. May, J. D. Fuentes, R. D. Cook, M. J. Gunsch, C. N. Mattson, R. S. Hornbrook, E. C. Apel and K. A. Pratt, *ACS Earth and Space Chemistry*, 2020, **4**, 1140–1148.

27 M. R. Albert, *Annals of Glaciology*, 2002, **35**, 52–56.

28 D. R. Bowling and W. J. Massman, *Journal of Geophysical Research*, 2011, **116**, G04006.

29 K. Toyota, J. C. McConnell, R. M. Staebler and A. P. Dastoor, *Atmospheric Chemistry and Physics*, 2014, **14**, 4101–4133.

30 J. L. Thomas, J. Stutz, B. Lefer, L. G. Huey, K. Toyota, J. E. Dibb and R. von Glasow, *Atmospheric Chemistry and Physics*, 2011, **11**, 4899–4914.

31 J. Cunningham and E. Waddington, *Atmospheric Environment. Part A. General Topics*, 1993, **27**, 2943–2956.

32 C. L. Clifton, Nisan. Altstein and R. E. Huie, *Environmental Science & Technology*, 1988, **22**, 586–589.

33 F. Domine, J. Bock, D. Voisin and D. J. Donaldson, *The Journal of Physical Chemistry A*, 2013, **117**, 4733–4749.

34 W. Liao and D. Tan, *Atmospheric Chemistry and Physics*, 2008, **8**, 7087–7099.

35 S. M. Clegg and J. P. D. Abbatt, *The Journal of Physical Chemistry A*, 2001, **105**, 6630–6636.

36 T. Bartels-Rausch, B. Eichler, P. Zimmermann, H. W. Gäggeler and M. Ammann, *Atmospheric Chemistry and Physics*, 2002, **2**, 235–247.

37 K. Tuite, J. L. Thomas, P. R. Veres, J. M. Roberts, P. S. Stevens, S. M. Griffith, S. Dusanter, J. H. Flynn, S. Ahmed, L. Emmons, S.-W. Kim, R. Washenfelder, C. Young, C. Tsai, O. Pikelnaya and J. Stutz, *Journal of Geophysical Research: Atmospheres*, 2021, **126**, e2021JD034689.

38 S. Ahmed, J. L. Thomas, K. Tuite, J. Stutz, F. Flocke, J. J. Orlando, R. S. Hornbrook, E. C. Apel, L. K. Emmons, D. Helmig, P. Boylan, L. G. Huey, S. R. Hall, K. Ullmann, C. A. Cantrell and A. Fried, *Journal of Geophysical Research: Atmospheres*, 2022, **127**, year.

39 M. Cesler-Maloney, W. Simpson, J. Kuhn, J. Stutz, J. Thomas, T. Roberts, D. Huff and S. Cooperdock, 2024, DOI: 10.5194/egusphere-2023-3082.

40 W. S. Goliff, W. R. Stockwell and C. V. Lawson, *Atmospheric Environment*, 2013, **68**, 174–185.

41 R. Von Glasow and P. J. Crutzen, *Atmospheric Chemistry and Physics*, 2004, **4**, 589–608.

42 H. Cho, P. B. Shepson, L. A. Barrie, J. P. Cowin and R. Zaveri, *The Journal of Physical Chemistry B*, 2002, **106**, 11226–11232.

43 A. Clifton, C. Manes, J.-D. Rüedi, M. Guala and M. Lehning, *Boundary-Layer Meteorology*, 2008, **126**, 249–261.

44 F. Domine, A.-S. Taillandier and W. R. Simpson, *Journal of Geophysical Research: Earth Surface*, 2007, **112**, 2006JF000512.

45 J. N. Crowley, M. Ammann, R. A. Cox, R. G. Hynes, M. E. Jenkin, A. Mellouki, M. J. Rossi, J. Troe and T. J. Wallington, *Atmospheric Chemistry and Physics*, 2010, **10**, 9059–9223.

46 U. Platt and J. Stutz, *Differential Optical Absorption Spectroscopy*, Springer Berlin Heidelberg, Berlin, Heidelberg, 2008.

47 A. C. Vandaele, P. C. Simon, J. M. Guilmot, M. Carleer and R. Colin, *Journal of Geophysical Research: Atmospheres*, 1994, **99**, 25599–25605.

48 S. Voigt, J. Orphal and JP. Burrows, *Journal of Photochemistry and Photobiology A: Chemistry*, 2002, **149**, 1–7.

49 B. Van Dam, D. Helmig, C. Toro, P. Doskey, L. Kramer, K. Murray, L. Ganzeveld and B. Seok, *Atmospheric Environment*, 2015, **123**, 268–284.

50 K. A. Murray, L. J. Kramer, P. V. Doskey, L. Ganzeveld, B. Seok, B. Van Dam and D. Helmig, *Atmospheric Environment*, 2015, **117**, 110–123.

51 Y. N. Lee and S. E. Schwartz, *The Journal of Physical Chemistry*, 1981, **85**, 840–848.

52 M. O. Sunday, L. M. D. Heinlein, J. He, A. Moon, S. Kapur, T. Fang, K. C. Edwards, F. Guo, J. Dibb, J. H. Flynn Iii, B. Alexander, M. Shiraiwa and C. Anastasio, 2024, DOI: 10.5194/egusphere-2024-3272.